

2

D-A235 677



DTIC

OFFICE OF NAVAL RESEARCH

Grant # N00014-90-J-1167

R&T Code 4133019

Technical Report # 12

Ionic Interactions in Electroactive Self-Assembled Monolayers of Ferrocene Species

by

Hugh C. De Long, John J. Donohue, and Daniel A. Buttry

Prepared for Publication in

Langmuir

Department of Chemistry
University of Wyoming
Laramie, WY 82071-3838

April 29, 1991

Reproduction in whole or in part is permitted for any purpose of the United States Government.

This document has been approved for public release and sale; its distribution is unlimited.

APR 29 1991
DTIC
A-1

01 5 08 038

Unclassified

SECURITY CLASSIFICATION OF THIS PAGE

REPORT DOCUMENTATION PAGE

1a. REPORT SECURITY CLASSIFICATION Unclassified			1b. RESTRICTIVE MARKINGS		
2a. SECURITY CLASSIFICATION AUTHORITY			3. DISTRIBUTION / AVAILABILITY OF REPORT Approved for public release and sale. Distribution unlimited.		
2b. DECLASSIFICATION / DOWNGRADING SCHEDULE			4. PERFORMING ORGANIZATION REPORT NUMBER(S) ONR Technical Report No. 12		
4. PERFORMING ORGANIZATION REPORT NUMBER(S) ONR Technical Report No. 12			5. MONITORING ORGANIZATION REPORT NUMBER(S)		
6a. NAME OF PERFORMING ORGANIZATION University of Wyoming		6b. OFFICE SYMBOL (if applicable)	7a. NAME OF MONITORING ORGANIZATION Office of Naval Research Resident Representative		
6c. ADDRESS (City, State, and ZIP Code) Department of Chemistry Univ. of Wyoming		Laramie, WY 82071-3838	7b. ADDRESS (City, State, and ZIP Code) University of New Mexico Bandelier Hall West Albuquerque, NM 87131		
8a. NAME OF FUNDING / SPONSORING ORGANIZATION Office of Naval Research		8b. OFFICE SYMBOL (if applicable) ONR	9. PROCUREMENT INSTRUMENT IDENTIFICATION NUMBER N 00014-90-J-1167		
8c. ADDRESS (City, State, and ZIP Code) 800 N. Quincy Street Arlington, VA 2217		10. SOURCE OF FUNDING NUMBERS	PROGRAM ELEMENT NO.	PROJECT NO.	TASK NO. R+T 413301901
11. TITLE (Include Security Classification) Ionic Interactions in Electroactive Self-Assembled Monolayers of Ferrocene Species		WORK UNIT ACCESSION NO.			
12. PERSONAL AUTHOR(S) H.C. DeLong, J.J. Donohue, and D.A. Buttry					
13a. TYPE OF REPORT Technical		13b. TIME COVERED FROM 9/90 TO 6/91	14. DATE OF REPORT (Year, Month, Day) 1991 April 29		15. PAGE COUNT 29
16. SUPPLEMENTARY NOTATION Accepted for publication in <u>Langmuir</u> .					
17. COSATI CODES			18. SUBJECT TERMS (Continue on reverse if necessary and identify by block number)		
FIELD	GROUP	SUB-GROUP	electrochemistry, self-assembled monolayer, quartz crystal microbalance.		
19. ABSTRACT (Continue on reverse if necessary and identify by block number)					
Abstract - The electrochemical and interfacial behavior of two types of electroactive self-assembled monolayer systems is investigated at gold electrodes. The first type is a ferrocene-based surfactant (a redox surfactant) derived from (dimethylamino)methylferrocene via quaternization of the amino group with various n-alkylbromides. These have a long alkyl chain with 16 or 18 carbons in the chain pendent from the cationic ammonium group. We refer to these as C16 and C18. The second type is a ferrocene-based dimeric species with a disulfide functional group capable of providing a permanent anchor to the Au electrode, thus endowing monolayers of this species with exceptional stability towards desorption. The electrochemical quartz crystal microbalance (EQCM) is used to monitor the mass changes which occur at the electrode surface during the redox processes of these two species. For the redox surfactants, we have previously shown that C12 and C14 (two shorter chain derivatives) desorb as a					
20. DISTRIBUTION / AVAILABILITY OF ABSTRACT <input checked="" type="checkbox"/> UNCLASSIFIED/UNLIMITED <input type="checkbox"/> SAME AS RPT <input type="checkbox"/> DTIC USERS			21. ABSTRACT SECURITY CLASSIFICATION Unclassified		
22a. NAME OF RESPONSIBLE INDIVIDUAL Daniel A. Buttry			22b. TELEPHONE (Include Area Code) (307) 766-6677		22c. OFFICE SYMBOL

consequence of oxidation. For C16 this same desorption occurs, but the rate is low enough to be monitored by changes in scan rate and depends on coverage. For C18, desorption following oxidation does not occur on the cyclic voltammetric timescale at room temperature, but does proceed at a measurable rate at elevated temperatures. For cases in which the desorption of the redox surfactant following oxidation is slow compared to the cyclic voltammetric scan rate, the EQCM results suggest that anion incorporation into the monolayer occurs prior to desorption. For the disulfide species, for which desorption following oxidation is not possible due to the strong Au-S interaction, the EQCM results suggest that reversible anion association with the monolayer occurs following oxidation to the ferricenium state. The conditions under which ions become incorporated into or associated with charged monolayers are discussed, as are some possible consequences of this phenomenon.

Ionic Interactions in Electroactive Self-Assembled Monolayers of Ferrocene Species

Hugh C. De Long^a, John J. Donohue^b, and Daniel A. Buttry^{*}

Department of Chemistry

University of Wyoming

Laramie, WY 82071-3838

Abstract - The electrochemical and interfacial behavior of two types of electroactive self-assembled monolayer systems is investigated at gold electrodes. The first type is a ferrocene-based surfactant (a redox surfactant) derived from (dimethylamino)methylferrocene via quaternization of the amino group with various n-alkylbromides. These have a long alkyl chain with 16 or 18 carbons in the chain pendent from the cationic ammonium group. We refer to these as C16 and C18. The second type is a ferrocene-based dimeric species with a disulfide functional group capable of providing a permanent anchor to the Au electrode, thus endowing monolayers of this species with exceptional stability towards desorption. The electrochemical quartz crystal microbalance (EQCM) is used to monitor the mass changes which occur at the electrode surface during the redox processes of these two species. For the redox surfactants, we have previously shown that C12 and C14 (two shorter chain derivatives) desorb as a consequence of oxidation. For C16 this same desorption occurs, but the rate is low enough to be monitored by changes in scan rate and depends on coverage. For C18, desorption following oxidation does not occur on the cyclic voltammetric timescale at room temperature, but does proceed at a measurable rate at elevated temperatures. For cases in which the desorption of the redox surfactant

following oxidation is slow compared to the cyclic voltammetric scan rate, the EQCM results suggest that anion incorporation into the monolayer occurs prior to desorption. For the disulfide species, for which desorption following oxidation is not possible due to the strong Au-S interaction, the EQCM results suggest that reversible anion association with the monolayer occurs following oxidation to the ferricenium state. The conditions under which ions become incorporated into or associated with charged monolayers are discussed, as are some possible consequences of this phenomenon.

a. Current address: Frank J. Seiler Research Laboratory, U.S. Air Force Academy, Colorado 80840-6528.

b. Current address: Lockheed Engineering and Sciences Company, P.O. Drawer MM, Las Cruces, New Mexico 88004

Introduction

The behavior of monolayer systems at electrode surfaces has been a topic of great interest to electrochemists for decades. A recent resurgence of interest in such systems stems in part from the potential they hold for allowing rational studies of structure-function relationships at electrode surfaces. The ability to control local topology at electrode surfaces offers the possibility of determining how geometric factors such as distance from the electrode, intermolecular packing, chirality, etc. conspire to determine the overall rates and thermodynamics of electron transfer reactions which occur there. For example, an electroactive self-assembled monolayer system based on the self-assembly of alkyl thiols has been described by Chidsey and coworkers (1). This system, which allows a ferrocene group to be placed and maintained at a controllable distance from the electrode surface, is designed to allow for detailed study of the distance dependence of electron transfer rates. Other, similar systems have been studied in the past (2,3), although the monolayers of these were structurally less well characterized. For systems of this type, the redox process involves changes in the charge of the redox group within the monolayer, raising the possibility of various types of ionic interactions which may influence either the rate or driving force of the electron transfer. In a previous contribution from our laboratory, it was demonstrated that ionic interactions can significantly influence the redox potentials and mutual interactions between redox groups within such electroactive self-assembled monolayers (4). This should be especially pronounced when the redox group is present at high coverage so that the areal charge density of the monolayer surface is high (5). In related work, it has been proposed that similar types of ion pairing interactions influence electron hopping rates in polymer films because of the necessity for ion motion during the activation event for the electron transfer (6). Thus, it appears that ionic interactions can play a role in determining electron transfer, especially in media with low local dielectric constants, and/or high volume or areal charge densities. As part of a continuing effort aimed toward understanding how molecular level

structural variations can influence redox processes at interfaces, we report here the behavior of several redox molecules which are capable of forming monolayer structures at Au (and other metal) electrode surfaces. The focus of this particular report is a study of the association of ionic species with these redox monolayers, where this association is driven by changes in the charge on the redox moiety by virtue of the redox process.

The molecules which were investigated in the present study are shown in Figure 1. The redox surfactants with 16 and 18 carbon chains pendent from the ammonium group are labeled as C16 and C18. The ferrocene derivative bearing the disulfide functionality is referred to as FcADS. We have previously shown that the shorter chain derivatives of the ferrocene-based redox surfactant are capable of adsorption onto Au electrodes, that the adsorption energy depends on the alkyl chain length, and that oxidation from the cationic Fe(II) species to the dicationic Fe(III) species causes desorption (5). In the present cases, the increased length of the alkyl chain slows down the electrochemically induced desorption process, so that for C16 and C18 the time course of these desorption events may be followed with the EQCM. Furthermore, clear evidence is presented for the presence of ionic interactions between anions from the supporting electrolyte and the charged ferricenium groups within monolayers of C16, C18, and FcADS.

Experimental

The syntheses of C16 ((ferrocenylmethyl)dimethylhexadecylammonium bromide) and C18 ((ferrocenylmethyl)dimethyloctadecylammonium bromide) followed a procedure previously described for shorter chain derivatives of the same type (5). FcADS was prepared by the following sequence of steps. First, ferrocene carboxylic acid was reacted with a slight molar excess of PCl_3 in benzene to give the acid chloride derivative. This was reacted in excess with 4-aminophenyl disulfide in CH_2Cl_2 . An excess of the acid chloride was used to ensure that both amino groups of the disulfide would be reacted. FcADS was collected as a

precipitate from the reaction mixture. All compounds were characterized by NMR. All chemicals were of reagent grade or better, and were used as received. Aqueous solutions were prepared using deionized water from a Millipore purification train. All potentials are quoted versus NaCl saturated SSCE.

The instrumentation for the EQCM measurements has been described in considerable detail elsewhere (5,7), as have the considerations pertinent to application of the EQCM to measurement of mass changes at electrode surfaces for species such as those studied here (5,7-9). We defer discussion of details to a later section, but point out that the EQCM is capable of detecting mass changes at the electrode surface by virtue of changes in its resonant frequency caused by these mass changes. As is the case for typical mechanical resonators, increases in frequency result from mass decreases and vice versa. In the present case, for the 5 MHz crystals used in this work, the proportionality constant relating frequency changes to mass changes is $56.6 \text{ Hz cm}^2 \mu\text{g}^{-1}$. Thus, a mass increase of $1 \mu\text{g}$ distributed over a 1 cm^2 area would give rise to a frequency decrease of 56.6 Hz. The experimental resolution for measurement of small frequency changes is ca. 0.1 Hz, this value being mainly determined by the stability of oscillation of the crystal/oscillator combination. Reproducibility is on the order of 0.2 Hz from experiment to experiment, so that frequency differences as small as 0.5 Hz are experimentally significant (see below).

Temperature dependent phenomena were examined in a non-isothermal, modified H-cell in which only the working compartment was thermostated with a Lauda constant temperature bath. Temperatures were controlled to within 0.02 degrees.

The EQCM and cyclic voltammetric (CV) data presented in the figures were typically the average of 5 scans. In some cases the data were digitally smoothed using a fourier transform smoothing routine which can result in minor distortion of the section of the voltammogram at which the scan direction is reversed. This is caused because the rapid current change on scan reversal transforms as a high frequency component of the signal, and

this component is altered by the fourier filter. However, these minor distortions in no way influence the interpretation of these data.

Solutions of the redox surfactants were prepared by direct addition of small aliquots of stock solutions of the redox surfactants to pure supporting electrolyte in the electrochemical cell. In all cases, sufficient time elapsed after addition to allow for adsorption equilibrium to be achieved prior to EQCM measurements, as judged by absence of further changes in the voltammetric response. At the small concentrations used in these experiments, it is probable that the true solution concentration of the redox surfactants is less than that calculated from the amount added due to adsorption of significant amounts of material onto the walls and frit of the cell. No correction for this effect was made. FcADS monolayers were assembled by exposure of the Au electrode to a saturated acetone solution of FcADS for periods ranging from a few minutes to a day. The concentration of this saturated solution was estimated to be near 10 μM . It was found that an exposure of one hour was sufficient to reach saturation coverage, as judged by the lack of further changes in the peak current of the ferrocene oxidation wave with longer exposure to the FcADS/acetone solution. Monolayers of FcADS which were roughly half-saturated (see below) were prepared by limiting the exposure time to ca. 20 minutes.

The surface roughness of the vacuum-deposited, thin film Au electrodes used in this work was 1.1 (10). This roughness was used in all calculations of surface coverages. These Au electrodes were prepared and stored in an oil-diffusion pumped high vacuum chamber (Edwards 306A), and were plasma etched in the chamber just prior to monolayer assembly. This procedure was found to greatly increase the reproducibility of the results.

Results and Discussion

Redox Surfactant Monolayers. Figure 2 shows the EQCM data for a typical scan across the redox wave of the ferrocene head group for C16 at a solution concentration of 8 μM . The

surface coverage at this concentration of C16 is 2.0×10^{-10} mole cm^{-2} , roughly two thirds of the surface coverage at saturation (3.2×10^{-10} mole cm^{-2}). At these low solution concentrations, the contribution to the voltammetric response from solution phase C16 is negligible, so only the surface wave for adsorbed C16 is observed. Quite similar behavior was previously described for the C12 and C14 derivatives (5,8,9), although their tendency towards adsorption is somewhat lower, so that larger concentrations are required to achieve similar surface coverages. The EQCM frequency data obtained during the voltammetric scan indicate a monotonic mass decrease during the oxidation of the adsorbed redox surfactant, behavior which is also similar to that observed for C12 (5,8,9) and C14 (5). Note that the anodic charge is larger than the cathodic charge, because of the desorption which occurs as a consequence of the oxidation process. Also, the replenishment of the surface population is slow because of the very low concentration, so the EQCM frequency does not return to its original value until after the termination of the scan. This discrepancy between anodic and cathodic charge depends inversely on scan rate and solution concentration and could, in principle, be used to calculate the rate of readsorption following rereduction of the redox surfactant. Potential step methods would probably be a better way of obtaining quantitative information on these processes. Temperature dependent measurements of desorption rates coupled with knowledge of the energetics of adsorption (see below) suggest that the readsorption process is essentially diffusion controlled (i.e. activationless). Thus, we have not pursued quantitative determination of readsorption rates, because they reveal little of about the interfacial behavior of these compounds.

The frequency increase in Figure 2 (6.3 Hz) is larger than the amount predicted for desorption of 2.0×10^{-10} mole cm^{-2} of C16 alone, which is 5.4 Hz. Discrepancies of this type were consistently observed at all surface coverages of C16, with the size of the discrepancy steadily increasing as the saturation coverage was approached. These discrepancies are suggestive of simultaneous loss of solvent and/or counterions (for the

cationic ammonium group) during desorption of C16. The magnitude of the discrepancy would be consistent with loss of one anion (H_2PO_4^- , in this case) for every redox surfactant molecule which desorbs, although other combinations of events are possible which would produce the same net mass change. In previous studies of the shorter chain derivatives (C12 and C14), similar evidence for association of ions with the monolayers was also observed (5).

Figure 3 shows the behavior of C16 at a concentration of 18 μM . At this concentration, the surface coverage is at its saturation value of 3.2×10^{-10} mole cm^{-2} . This value is consistent with previous determinations of the saturation coverages of C12 (5,8,9) and C14 (5), and corresponds to a molecular area of 50 \AA^2 per molecule. This is also the area of the head group of this surfactant species comprised of the ammonium and ferrocenyl groups, as determined by Facci from Langmuir trough measurements on longer chain ferrocene derivatives (11) and from molecular models. These results imply that the saturation coverage is determined by close-packing of this head group. We have no experimental information on the relative orientation of these surfactants (i.e. head up versus head down). However, we favor the head up orientation because, if they were head down, it is not clear why the monolayer would not prefer an interdigitated, bilayer-like structure (which would exhibit a charge more than twice that observed here) to minimize hydrophobic interactions with the aqueous solution (9). Also note that in all cases the applied potential is positive of the potential of zero charge on Au (12), so that there is electrostatic repulsion between the metal surface and the redox surfactants.

The CV data reveal a larger anodic charge than that for the lower concentration. Also, the anodic and cathodic charges are nearly equal. Further, the EQCM data now show a transient mass gain (frequency decrease) during the initial stages of the oxidation process, followed by slow mass loss during the remainder of the oxidation. Readsorption does not occur until a significant fraction of the C16 has been reduced back to the Fe(II) state, as occurred at the lower concentration shown in Figure 2. These data suggest that desorption of

the dicationic species produced by C16 oxidation is slow, and that transient anion and/or solvent incorporation occurs prior to the desorption of the oxidized monolayer. Presumably, anion incorporation during oxidation occurs to compensate some of the cationic charge created on the ferrocene moiety. Thus, as was observed for the viologen self-assembled monolayers previously described (4), anion transport out of or into the monolayer seems to occur in such a way as to compensate for the injection or removal of electrons, respectively. However, there is an important caveat to this which will be discussed below.

Figure 4 presents data which are supportive of the above interpretation. These are EQCM frequency data obtained during CV scans at 10, 50, and 250 mV s^{-1} for a C16 solution concentration (15 μM) at which the surface coverage is at its saturation value. At the fastest scan rate, the transient mass gain is the largest. At an intermediate scan rate the transient mass gain is still in evidence, but is of diminished magnitude. At the slowest scan rate, no transient mass gain is observed. Instead, smooth mass loss following oxidation and mass regain during reduction is observed, much like the behavior of C16 at lower surface coverages or shorter chain derivatives (C10, C12, and C14) at any surface coverage. Thus, it appears that the desorption rate for these redox surfactants depends not only on chain length, but also on surface coverage.

Figure 5 shows the behavior for the C18 derivative present in solution at a concentration of 5 μM . The anodic and cathodic charges are now seen to be equal, and instead of mass loss during oxidation, mass gain is observed. The magnitude of the frequency decrease during the oxidation is about 4 Hz, considerably larger than the roughly 0.8 Hz decrease expected for the incorporation of enough H_2PO_4^- to neutralize all of the cationic ferricenium sites created during the oxidation. It seems likely that additional solvent association with the monolayer also occurs following oxidation, and that the unexpectedly large mass gain is due to the mass of this additional solvent. At any rate, these data are consistent with the interpretation that C18 does not desorb to any significant extent during its

oxidation at room temperature (ca. 20 - 22 °C in our labs). Rather, anion and/or solvent incorporation into the monolayer seem to occur as was indicated for the C16 derivative at surface coverages near the saturation value.

Figure 6 shows the EQCM frequency data obtained for similar scans over the ferrocene wave at elevated temperatures. Curve A shows the desorption behavior at 30 °C, and curve B shows the desorption behavior at 50 °C. Clearly, the desorption rate is increased at elevated temperatures, so that at 50 °C loss of the redox surfactant from the surface is nearly complete during the course of the voltammetric scan (a timescale of roughly 15 seconds), while at 30 °C the desorption requires about twice as long.

Increases in the solution concentration of C18 to 25 μM lead to adsorption of multilayer amounts of the redox surfactant onto the surface. This is shown in Figure 7. Here the anodic charge for the voltammetric scan corresponds to roughly 5 equivalent monolayers of C18. The EQCM data also show desorption of a considerable amount of C18 during the oxidative scan, with the mass change calculated from the frequency increase again consistent with desorption of roughly 5 equivalent monolayers of C18. Repeated cycling over the wave at this concentration eventually leads to a voltammetric response which is similar to that shown in Figure 5, but with slightly larger peak currents and charges. Thus, formation of multilayers is possible, but the layer of redox surfactant in direct contact with the electrode seems to be considerably more stable toward redox cycling than those farther away.

FcADS Monolayers. Figure 8 shows the CV and EQCM responses of a monolayer of FcADS in a solution of pure supporting electrolyte (0.1 M HClO_4) which contains no FcADS. These data are the average of 10 scans, where the number of scans was increased because of the very small magnitude of the EQCM frequency change. The redox process for the ferrocene moiety is clearly observed, and the anodic and cathodic charges are equal. This voltammetric response is observed for many (more than 100) cycles, indicating that the FcADS monolayer

is stably attached to the Au electrode. The large separation between the anodic and cathodic current peaks is not a result of diffusional limitations for the redox process, but rather a reflection of either slow kinetics or non-ideal behavior. We have not investigated this further. The surface coverage calculated from the charge in the scan is 3.0×10^{-10} mole cm^{-2} . This gives a molecular area for the adsorbed molecule of 55 \AA^2 per molecule. As discussed above, the ferrocene head group has a projected area of 50 \AA^2 per molecule (5,9), so the observed area is consistent with formation of a close-packed monolayer at a coverage very near to saturation.

The EQCM data indicate mass gain during oxidation and mass loss during reduction, as was observed for C18 at low temperatures. However, the magnitude of the frequency change is roughly half of the 1.8 Hz value expected for insertion of 3.0×10^{-10} mole cm^{-2} of ClO_4^- anions into the monolayer during the oxidation. There are at least two possible explanations for this type of behavior. The first possibility is that cation and/or solvent expulsion from the monolayer occur simultaneously with anion insertion during oxidation (and vice versa during reduction), so that the observed, net mass change is decreased from the "anion only" value. This seems unlikely because the hydrophobic nature of the monolayer coupled with the high surface coverage and consequent steric congestion in the monolayer mitigate against incorporation of large quantities of solvent and/or cations. In addition, the applied potential in these experiments is quite positive of the point of zero charge of Au (12), so that incorporation of cations into the monolayer should be unfavorable on electrostatic grounds. The second possibility is that the anions do not actually enter the monolayer, but rather some fraction of them becomes closely associated with it in the solution immediately adjacent to the monolayer (see Conclusions section). This seems more reasonable since the steric congestion caused by close-packing should inhibit penetration of anionic species into the monolayer. Note that the situation with the FcADS monolayer is significantly different than that with the redox surfactants. FcADS is both anchored and rigid while the redox

surfactants are free to move about on the surface as well as assume a large number of possible conformational states. Further, the FcADS monolayers are adsorbed with the molecule in its neutral, Fe(II) state. Thus, there is no requirement for counterion incorporation during assembly of the monolayer, so that packing of the adsorbate should be more efficient. These arguments suggest that penetration of anions and solvent into the redox surfactant monolayers should be much more facile than into the FcADS monolayers.

To further probe the influence of steric congestion on the ability of solvent and/or ions to enter these monolayer structures, we examined the behavior of FcADS at two different surface coverages (i.e. saturation, $3.0 \times 10^{-10} \text{ mol cm}^{-2}$, and near half saturation, $1.6 \times 10^{-10} \text{ mol cm}^{-2}$) in 0.1 M NaCl. A solution containing Cl^- was used because previous results on a viologen self-assembled monolayer revealed that solvent molecules accompanied Cl^- into and out of the monolayer during redox cycling of the viologen redox moieties (4), and it was expected that solvent transport would be sensitive to steric congestion. The data for these experiments are shown in Table 1. Also shown are values of MW_{app} which is the apparent molecular weight of the species undergoing transport. It is calculated from the electrochemical charge and the frequency (mass) change during oxidation, and can be thought of as the mass which is transported for each electron extracted from the monolayer (7,13). In a solution containing Cl^- , MW_{app} would have a value of 35.5 g mol^{-1} if the oxidation caused incorporation of exactly one anion for each electron extracted. The extent to which MW_{app} is different from 35.5 reveals either a mixed transport situation in which solvent and/or cation transport accompanies anion transport or the situation described above in which only a fraction of the anions associate with the charged monolayer. In this latter case, the measured mass change may be considerably less than expected, as discussed below.

The value of MW_{app} for saturation coverage is ca. 30% less than expected for Cl^- , while the value for half coverage is very much larger. The value for saturation coverage is not inconsistent with the discussion above. On the other hand, the value for half coverage is far

too large to be accounted for by the simple incorporation of hydrated Cl^- into the monolayer. It is possible to rationalize this finding by assuming that the adsorbed species are in a highly tilted arrangement in the reduced form, but assume a more perpendicular orientation following oxidation, a process which might be driven by the much stronger solvation of the hydrophilic ferricenium group as compared to the hydrophobic ferrocene group. In this scenario, the achievement of a nearly perpendicular orientation would be accompanied by an influx of solvent into the monolayer, leading to a much larger value for MW_{app} than predicted for Cl^- transport alone.

An alternative explanation for this observation is that the transformation of the monolayer from hydrophobic to hydrophilic causes a dramatic change in the acoustic coupling between the electrode surface and the solution (7). We are currently investigating methods to test this hypothesis.

Whatever the cause of the deviations of the frequency changes from those expected from the (rather simplistic) models presented above, it seems clear that the creation of cationic sites within monolayers of FcADS leads to relatively strong association of supporting electrolyte anions with these newly created, charged sites. Further evidence for such anionic association is found in the shifts observed for the formal potential of FcADS in solutions containing different anions. For example, formal potentials of 0.49 , 0.54, and 0.59 V were observed for a monolayer of FcADS transferred successively between solutions of HClO_4 , , HNO_3 , and H_2SO_4 , all at concentrations of 1.0 M. A reasonable interpretation of these data is that the stabilization of the ferricenium group in the FcADS monolayer by ion pairing occurs in the order $\text{ClO}_4^- > \text{NO}_3^- > \text{HSO}_4^-$. Creager (14) has recently observed similar evidence for strong ion pairing between ClO_4^- and ferrocene groups in a self-assembled system similar to that described by Chidsey et al. (1).

Conclusions

The results presented here have shown that the desorption rates of the C16 and C18 redox surfactants depend on both the chain length and the surface coverage, with lower rates resulting from higher coverage and/or longer chain lengths. These observations are also qualitatively in agreement with Facci's early study of the essentially irreversible adsorption of the C18 derivative onto Pt electrodes from acidic sulfate and perchlorate solutions (11). For physically (as opposed to chemically) adsorbed molecules of this type it is generally accepted that the activation energy for adsorption is essentially zero, so that the activation energy for desorption should be roughly equal to the adsorption energy (15). We have previously determined the adsorption energies of the C10, C12, and C14 derivatives of this class of redox surfactants (5). The adsorption energy for the oxidized form of C14 is -27 kJ mol^{-1} , so the value for the oxidized form of C18 should be in the range -28 to -32 kJ mol^{-1} . If this is taken as an estimate of the activation energy for desorption, then it is possible to calculate the expected ratio of half-lives for desorption at two different temperatures, assuming simple Arrhenius behavior. This calculation predicts that desorption should take about twice as long at $30 \text{ }^\circ\text{C}$ than it does at $50 \text{ }^\circ\text{C}$, which is in qualitative agreement with the data in Figure 6. Thus, the picture which develops is one in which the desorption process is activated, with an activation energy similar to the adsorption energy. That the desorption rate for C16 is coverage dependent is also not unexpected, because at increased coverage attractive lateral interactions should begin to contribute to the activation energy for desorption (15).

For cases in which changes in surface populations of the redox species are negligible during the CV timescale, either because of slow desorption (C16 and C18) or irreversible adsorption (FcADS), EQCM measurements of the compositional changes which occur within these electroactive self-assembled monolayers during redox cycling have provided convincing evidence that the creation of charge within a monolayer assembly can drive counterions to associate with or incorporate into monolayer structures. Similar effects have

previously been observed in thin films of redox active polymers (16,17). In the case of self-assembled monolayer structures, steric congestion may significantly inhibit complete insertion of charge compensating ions. This inhibition could result in large, relatively unscreened repulsive interactions between like-charged redox groups within the monolayer, leading to a host of unusual effects including broad voltammetric waves. Also, the permanent presence of the redox moiety within the potential gradient at the electrode surface (i.e. in the space charge region) could lead to unusual thermodynamic effects (18), and influence the degree of counterion association (see below).

It has been known for some time that counterions can associate with charged species in Langmuir-Blodgett monolayers, vesicles, micelles, and bilayers (19-31). These associations change the properties (such as charge, surface potential, diffusivity, etc.) of these assemblies in a way that is easily detectable by a wide range of measurements. In the present context, so little is known about the manner in which the EQCM interacts with species which are closely associated with, but not completely incorporated into, surface assemblies, that it is difficult to predict the expected magnitudes of the frequency changes for such processes. Thus, quantitative interpretation of these effects must await the development of more sophisticated models for the interaction of the EQCM with the adjacent solution. Nevertheless, these data and the data for the C18 redox surfactant give clear, if only semiquantitative, indications of the association of counterions with these self-assembled monolayers when they have large areal charge densities due to the presence of large numbers of charged (redox) species within the monolayer.

Several detailed theoretical treatments of ionic association at the surface of charged aggregates have been recently described, with that by Ruckenstein and Beunen (21) being one of the more lucid. They give a measure of these ionic interactions in the form of a degree of dissociation, α , which measures the fraction of charged surface groups which do not have bound counterions. Their theoretical estimates of this quantity for sodium dodecylsulfate

(SDS) micelles range from 0.05 to 0.3 depending on the values of various parameters which can influence α , the most important of which seem to be the dielectric constant near the charged surface (which may be much different than that in the bulk), salt concentration, and the area per head group (i.e. the areal charge density). Experimental values for α for the SDS and related micellar systems range from 0.14 (29) to as high as 0.5 (30), depending on the method of its determination. We also note that α values for lithium, sodium, and cesium dodecylsulphate micelles are 0.73, 0.49, and 0.31, respectively (31), indicating that the identity of the counterion can have a dramatic influence on the degree of dissociation.

It is tempting to assert that our observations of frequency changes which are less than predicted for complete association of counterions with these charged monolayer assemblies are related to the fact that some of the charged sites have completely associated counterions while others are dissociated. In fact, it is possible that our EQCM measurements can provide a measure of α for these charged monolayers, if only the associated ions are sensed by the vibrating quartz transducer. However, we hesitate to make quantitative calculations based on this premise until such time as more detailed experiments have been conducted to test the hypothesis, such as dependence on ionic strength and different ion types. At any rate, the important points here are that a wide range of α values may be expected for different experimental conditions, and that the expected values are not at odds with our observations.

The data presented in this paper also point to the electrochemically induced modulation of the degree of association of solvent with these self-assembled monolayer systems. Previous results from this laboratory led to the same conclusion for a self-assembled viologen monolayer system (4). These observations of changes in both ion and solvent association with self-assembled monolayer systems are especially significant because of the projected use of such systems for detailed investigation of distance dependent electron transfer rates. These studies usually seek to compare and contrast solution phase data with monolayer data. The present observation of the creation of charge within the monolayer

structure causing strong counterion association with the monolayer constitutes an important caveat to such efforts. In this context, it will be especially important to measure, and hopefully understand, such solvent and ionic associations because they can dominate the kinetics of electron transfer processes for redox groups which are grafted into self-assembled monolayer structures, just as they influence electron transfer events in redox polymers (6).

Acknowledgements - We are grateful for the Office of Naval Research for the full support of this work.

References

1. Chidsey, C.E.D.; Bertozzi, C.R.; Putvinski, T.M.; Mujisce, A.M. J. Am. Chem. Soc., 1990, 112, 4301-36.
2. Li, T.-T.; Liu, H.-Y.; Weaver, M.J. J. Am. Chem. Soc., 1984, 106, 1233-39.
3. Li, T.-T.; Weaver, M.J. J. Am. Chem. Soc., 1984, 106, 6107-08.
4. De Long, H.C.; Buttry, D.A. Langmuir, 1990, 6, 1319-22.
5. Donohue, J.J.; Buttry, D.A. Langmuir, 1988, 5, 671-78.
6. a) Saveant, J.-M. J. Phys. Chem., 1988, 92, 4526-32. b) Saveant, J.-M. J. Phys. Chem., 1988, 92, 1011-13.
7. Buttry, D.A. In Electroanalytical Chemistry; Bard, A.J., Ed.; Marcel Dekker: New York, 1991; Vol. 17, pp. 1-85.
8. Donohue, J.J.; Nordyke, L.L.; Buttry, D.A. In Chemically Modified Surfaces in Science and Industry; Leyden, D., Collins, W., Eds.; Gordon and Breach: New York, 1988, pp. 377.
9. Nordyke, L.L.; Buttry, D.A. Langmuir, 1991, 7, 380-8.
10. De Long, H.C.; Buttry, D.A., unpublished results.
11. Facci, J.S. Langmuir, 1987, 3, 525-9.

12. The point of zero charge (pzc) of bare gold is ca. -0.2 to 0.0 V vs SSCE, which is well negative of the formal potential of the ferrocene moieties in these monolayers. See, for example, Silva, F.; Sottomayor, M.J.; Hamelin, A. J. Electroanal. Chem., 1990, 294, 239-51, and references therein.
13. Ostrom, G.S.; Buttry, D.A. J. Electroanal. Chem., 1988, 256, 411-31.
14. S. Creager, personal communication.
15. Adamson, A. "Physical Chemistry of Surfaces"; Wiley and Sons: New York, 1976; Chapter 15.
16. Varineau, P.T.; Buttry, D.A. J. Phys. Chem., 1987, 91, 1292-95.
17. Borjas, R.; Buttry, D.A. J. Electroanal. Chem., 1990, 280, 73-90.
18. S. Feldberg, personal communication.
19. Brady, J.E.; Evans, D.F.; Warr, G.G.; Grieser, F.; Ninham, B.W. J. Phys. Chem., 1986, 90, 1853-59.
20. Evans, D.F.; Sen, R.; Warr, G.G. J. Phys. Chem., 1986, 90, 5500-02.
21. Ruckenstein, E.; Beunen, J.A. Langmuir, 1988, 4, 77-90.
22. Rathman, J.F.; Scamehorn, J.F. Langmuir, 1987, 3, 372-7.
23. Kale, K.H.; Zane, R. J. Colloid Interfac. Sci., 1977, 61, 312-19.
24. Abuin, E.; Lissi, E.; Backer, E.; Zannoco, A.; Whitten, D. J. Phys. Chem., 1989, 93, 4886-90.
25. Cuccovia, I.M.; Chaimovich, H.; Lissi, E.; Abuin, E. Langmuir, 1990, 6, 1601-04.
26. Fendler, J.H.; Hinze, W.L. J. Am. Chem. Soc., 1981, 103, 5439-43.
27. Moss, R.A.; Ihara, Y.; Bizzigotti, G.O. J. Am. Chem. Soc., 1982, 104, 7476-80.
28. Marra, J. J. Phys. Chem., 1986, 90, 2145-50.
29. Mysels, K.J.; Princen, L.H. J. Phys. Chem., 1959, 63, 1696.
30. Anacker, E.W. in "Solution Chemistry of Surfactants"; Mittal, K. Ed.; Plenum, New York, 1979; Vol. 1, pp. 247-265.

31. Frahm, J.; Diekmann, S.; Haase, A. Ber. Bunsenges. Phys. Chem., 1980, 84, 566-71.

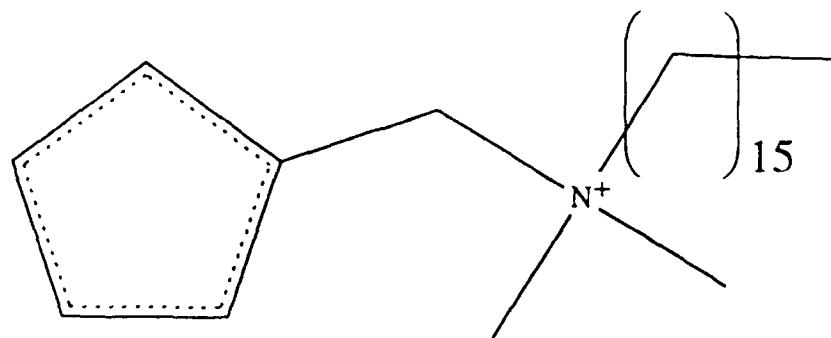
Table 1

Effect of Surface Coverage on Mass Transport within the Monolayer for FcADS

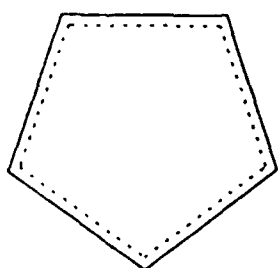
Surface Coverage (mol cm ⁻²)	Δf (Hz)	MW _{app} (g mol ⁻¹)
1.6 x 10 ⁻¹⁰	3.65	410
3.0 x 10 ⁻¹⁰	0.44	25

Figure Captions

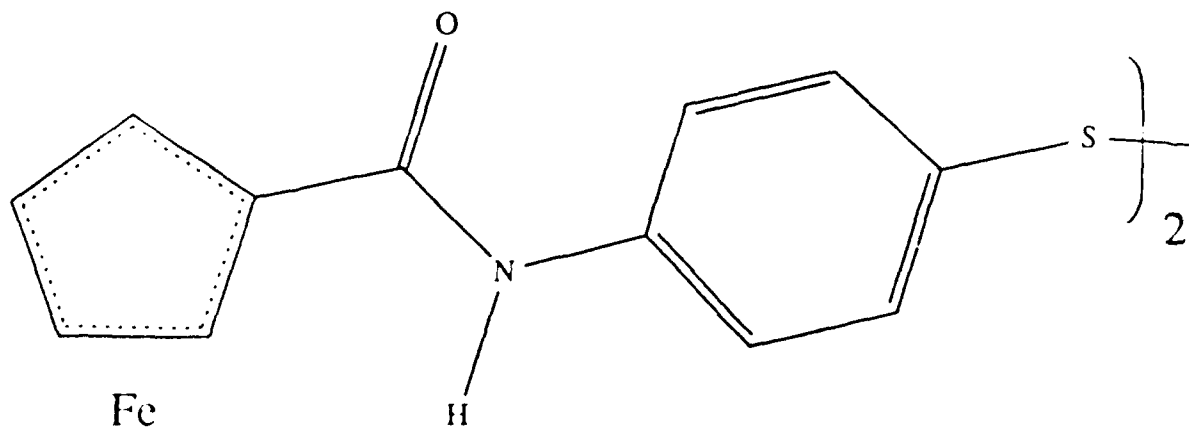
1. The structures of C16 and FcADS.
2. EQCM scan for 8 μM C16 in 0.2 M H_3PO_4 , scan rate 50 mV s^{-1} . A) CV. B) EQCM frequency.
3. EQCM scan for 18 μM C16. All other conditions as in Figure 2.
4. EQCM frequency data for three separate scans in a solution containing 15 μM C16. All other conditions as in Figure 2, except scan rate which is A) 10 mV s^{-1} , B) 50 mV s^{-1} , and C) 250 mV s^{-1} .
5. EQCM scan for 5 μM C18. All other conditions as in Figure 2.
6. EQCM frequency data for two separate scans in a solution containing 5 μM C18 at two different temperatures.: A) 30 $^\circ\text{C}$, and B) 50 $^\circ\text{C}$.
7. EQCM scan after exposure to a 25 μM of C18 in 0.2 M H_3PO_4 for one hour. All other conditions as in Figure 2.
8. EQCM scan for a FcADS monolayer in 1.0 M HClO_4 at a scan rate of 100 mV s^{-1} .



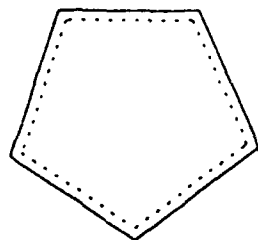
Fe



C16



Fe



FeADS

